

Robotized measurements for geometric and acoustic characterization of unknown structures

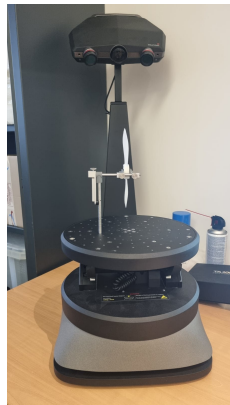
Caroline PASCAL

U2IS & UME – ENSTA Paris

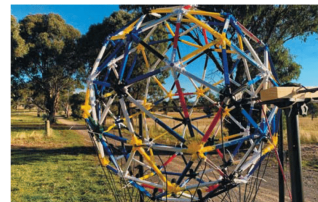
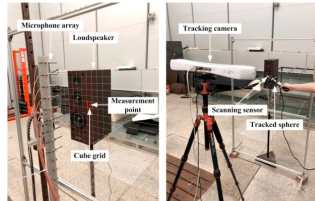
November 21, 2023



Introduction - Context



Geometric measurements [1]



Acoustic measurements [2][3]

⇒ Measurements and metrology operations are often **tedious**,
time-consuming and **unadaptable**.

Introduction - Objectives

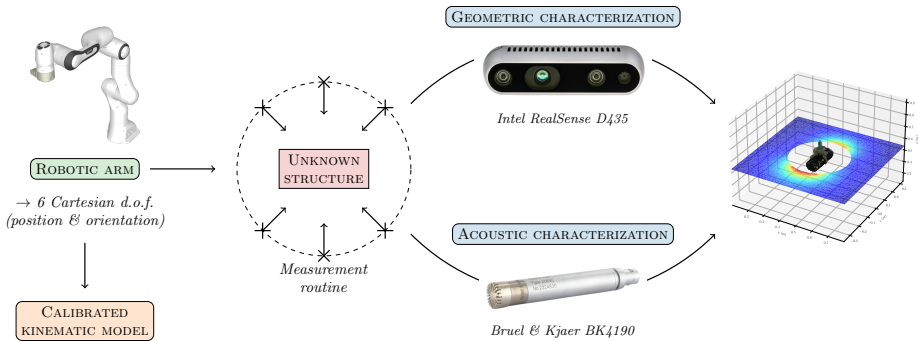


Table of Contents

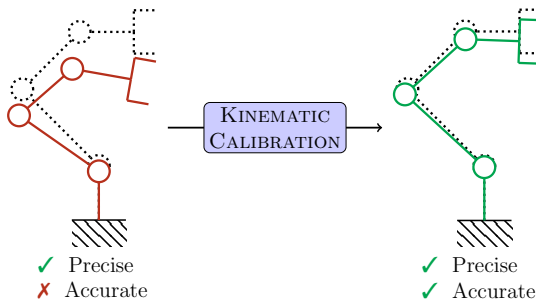
- 1 Introduction - Context and objectives
- 2 Robotic arm kinematic calibration - Accuracy improvement
- 3 Geometric characterization - 3D scan
- 4 Acoustic characterization - Acoustic field reconstruction
- 5 Conclusion & discussion

Table of Contents

- 1 Introduction - Context and objectives
- 2 Robotic arm kinematic calibration - Accuracy improvement
- 3 Geometric characterization - 3D scan
- 4 Acoustic characterization - Acoustic field reconstruction
- 5 Conclusion & discussion

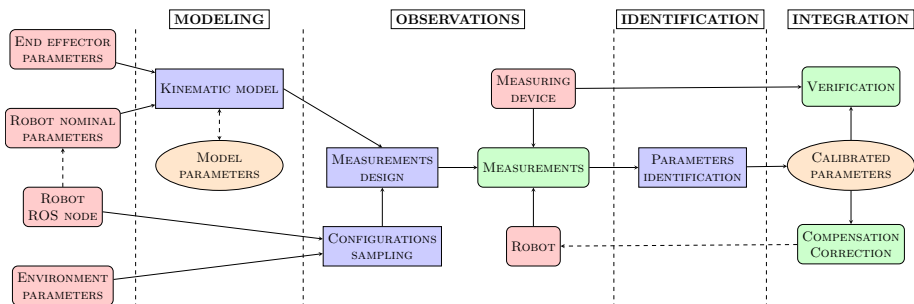
Robot arm kinematic calibration [4]

→ **Initial assessment** : Serial robots have a *high positioning repeatability* but a *poor absolute accuracy*.



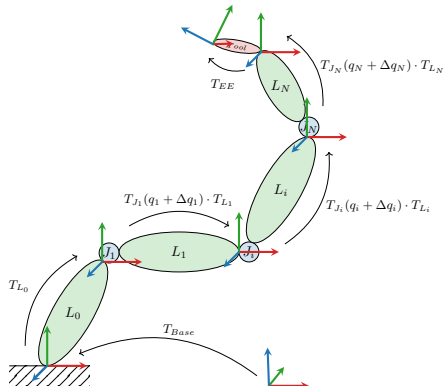
→ **Aftermath assessment** : There is no complete and off-the-shelf kinematic calibration tool !

Step 1 : Define a kinematic calibration procedure



Description of the overall kinematic calibration procedure

Modeling (1)



Seeked model properties

- **Faithfullness** : Compliance with the robot true behaviour;
- **Completeness**, but without any **redundancy** : Model defined by a determined set of parameters;
- **Continuity** : Continuous function of the parameters;

Modeling (2)

Full-pose geometric modeling

$$\begin{aligned} T(q, \pi) = & T_{Base}(\pi_{Base}) \cdot T_{Link_0}(\pi_{L_0}) \\ & \cdot [T_{Joint_1}(q_1 + \Delta q_1, \pi_{J_1}) \cdot T_{Link_1}(\pi_{L_1})] \dots \\ & \cdot [T_{Joint_N}(q_N + \Delta q_N, \pi_{q_N}) \cdot T_{Link_N}(\pi_{L_N})] \cdot T_{EE}(\pi_{EE}) \end{aligned}$$

Where $\pi = (\pi_{Base}, \pi_{J_i}, \pi_{L_i}, \pi_{EE})$ are the *kinematic model parameters*

Partial-pose geometric modeling [5][6]

$$\begin{aligned} (P^i(q, \pi))_{i=1\dots M} = & T_{Base}(\pi_{Base}) \cdot T_{Link_0}(\pi_{L_0}) \\ & \cdot [T_{Joint_1}(q_1 + \Delta q_1, \pi_{J_1}) \cdot T_{Link_1}(\pi_{L_1})] \dots \\ & \cdot [T_{Joint_N}(q_N + \Delta q_N, \pi_{q_N}) \cdot T_{Link_N}(\pi_{L_N})] \cdot T_{EE_i}(\pi_{EE_i}) \Big|_P \end{aligned}$$

Where EE_i refers to the end effector point $i \in \{1\dots M\}$

Modeling (3)

Redundancy elimination for revolute joints [7]

→ If the current and previous joints are **colinear**

 ⇒ Remove the closest translation orthogonal to the common rotation axis among the previous links transformations.

 + **Base** and **Tool** transformations simplification.

→ If the current and previous joints are **orthogonal**

 ⇒ Remove the rotation in the previous link transformation corresponding to the current joint rotation axis.

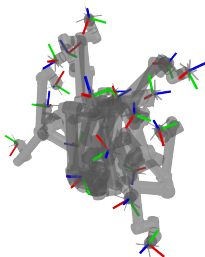
Observations

→ Open-loop observations, using internal monitoring (joints encoders) and external measurements (end effector points positions).

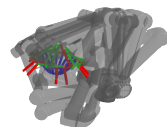
→ *How to pick the measured robot configurations ?*

- ① Perform a reachable and task-oriented sampling of the robot workspace [8];

Random sampling



3D scan inspired sampling



- ② Choose the configurations maximizing parameters O_1 identifiability using combinatorial optimization [9].

Positioning accuracy optimization

$$\pi^* = \arg \min_{\pi} \sum_{i=1}^{N_{\text{meas}}} \sum_{j=1}^{N_{EE}} \underbrace{\left\| P^j(q_i, \pi) - P_{\text{measured}}^j(q_i) \right\|^2}_{\epsilon_i^j}$$

Where ϵ_i^j defines the *positioning error* of the end effector point j for the i -th measurement.

→ The sum of **positionning errors** over all end effector points and measurement configurations defines the **robot accuracy**.

Integration

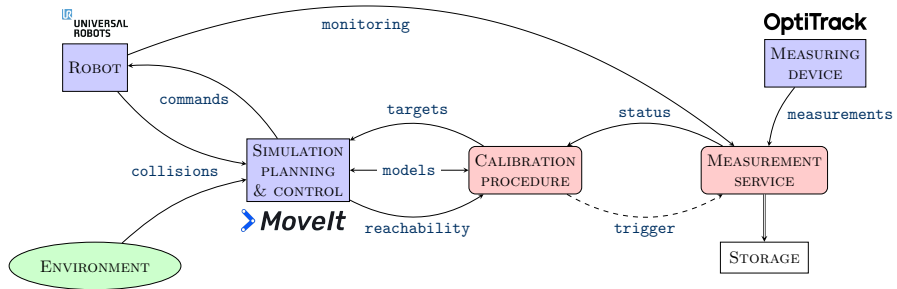
Verification

→ Validate the calibrated parameters with the accuracy obtained on a new set of randomly picked measurements.

Integration

- Compensation: Integrate the calibrated parameters directly in the robot controller.
- Correction : Build a new robot description with the calibrated parameters.

Step 2 : Handle the hardware-software interfaces



Description of the hardware-software interfaces

Robot integration

→ *Movelt* motion planning framework API
+ custom overlay : `robot_arm_tools`

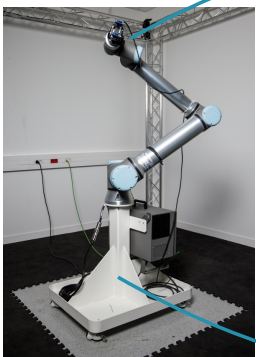
Simulation

- *Collision* and *singularity* aware motion planning tool, providing *reachability* insights;
- *Modular* yet *generic* planning and kinematic pipelines, *with* custom constraints;
- A simplified definition and integration of common use-cases;

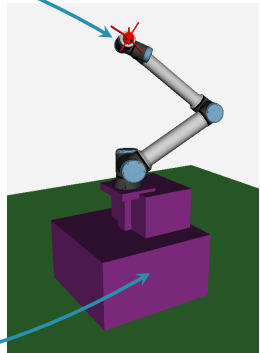
Real robot

- *User-friendly* and *high-level* integration of real robots ROS controllers;
- Dynamic interruption and low-level recovery of motion execution;
- A logging solution to monitor and recover multiple waypoint trajectory execution.

External environment integration



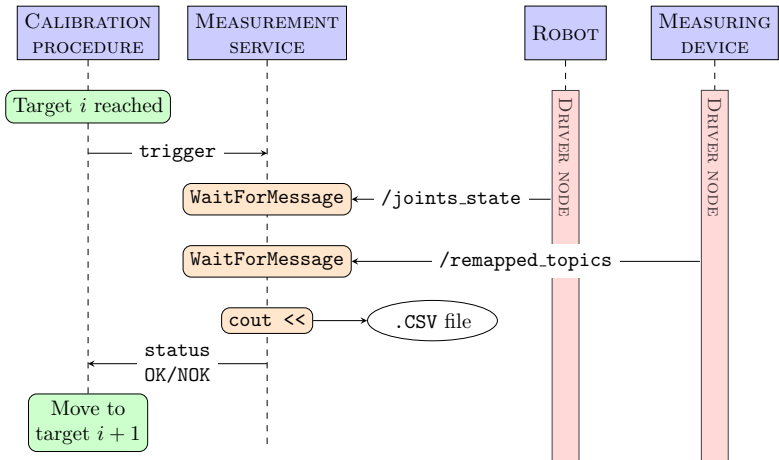
Automated URDF/XACRO
generation from
STL mesh file
→ /robot_description
tweakage



User defined YAML file
with basic
geometric primitives
→ moveit_visual_tools
overlay

Measuring devices integration

→ Creation of a generic ROS service *MeasurementService* for motion and measurements synchronization.



Experimental validation setup - Robots



Universal Robots - UR10e

- 6 axis
- 18 geometric parameters



Franka Emika - Panda

- 7 axis
- 22 geometric parameters

+ 6 Base and $3 \times M$ Tool parameters

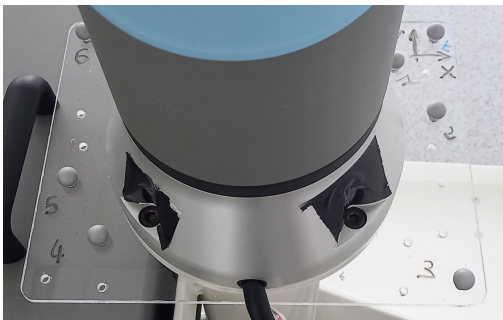
Experimental validation setup - External measuring device

→ Optitrack position tracking tool.



→ 6 *Prime 13* cameras
⇒ ±0.2 mm accuracy.

Experimental validation setup - Measurements bodies



→ Robot base and end effector points measurements bodies.
 $M = 7$ reflective spheres in a precise 3D layout.

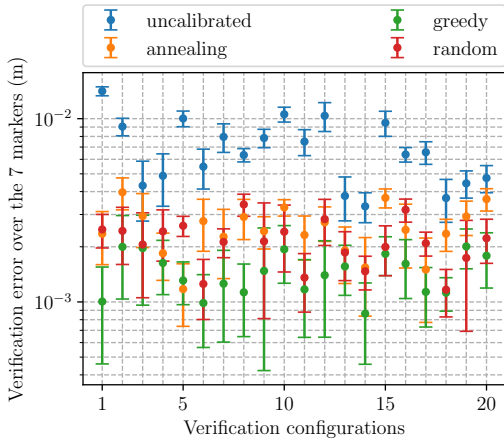
Example of calibration measurements



Calibration measurements of an UR10e (speed $\times 2$)

Experimental validation - Results (Panda)

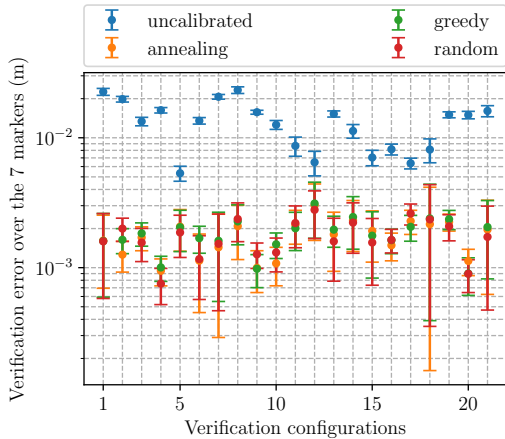
	F.E. Panda
Total parameters	49
Measurements configurations	98
Overall duration (h)	4.38
Modeling (min)	55
Measurements (h)	3.1
Identification (min)	22
Initial accuracy (mm)	7.66
Best final accuracy (mm)	1.63
Improvement rate	78.7%



Average positioning errors over the 7 markers with and without calibration

Experimental validation - Results (UR10e)

UR10e	
Total parameters	45
Measurements configurations	90
Overall duration (h)	7.03
Modeling (min)	45
Measurements (h)	6.0
Identification (min)	17
Initial accuracy (mm)	14.4
Best final accuracy (mm)	2.03
Improvement rate	85.9%



Average positioning errors over the 7 markers with and without calibration

Projected work and perspectives

- Allow full-pose and indirect measurements
 - ↪ In particular, investigate the combined camera-robot calibration opportunity.
- Increase measurements robustness
 - ↪ Avoid robot induced obstructions while selecting measurements configurations, strengthen measurement redundancies.
- Introduce actuator flexibilities and backlash in the kinematic model
 - ↪ Take the effects of gravity on the robot actuators into account [10], especially for heavy tools and sensors.

Table of Contents

- 1 Introduction - Context and objectives
- 2 Robotic arm kinematic calibration - Accuracy improvement
- 3 Geometric characterization - 3D scan
- 4 Acoustic characterization - Acoustic field reconstruction
- 5 Conclusion & discussion

Geometric characterization: context and motivation

→ An already tackled issue...



Example of robotized 3D scan setup :
RoboScan [11]

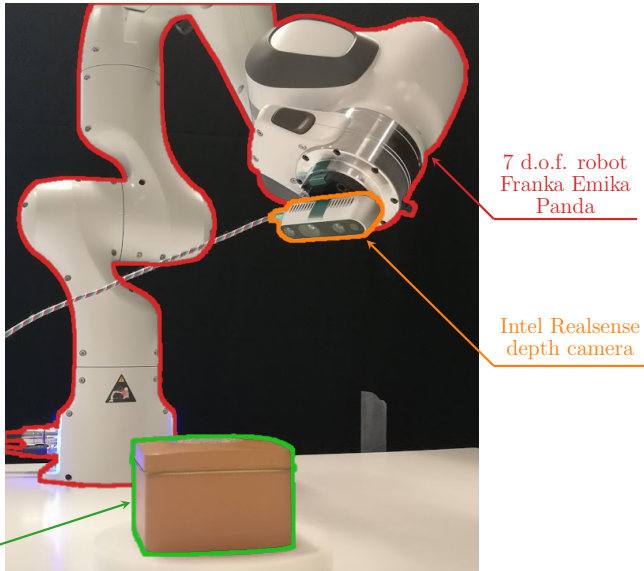
→ ...In various robotics fields.



Example of an outdoor RTABMAP 3D
cartography [12]

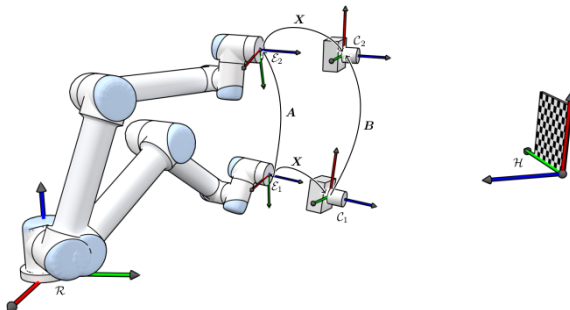
⇒ **Objective** : Retrieve the studied object *3D part* and *relative position* to the robot.

Robotized geometric measurements setup



Preliminary work : hand-eye calibration

⇒ **Goal** : Find the transformation between the robot flange and the camera optical center.



Credits : Torstein A. Myhre

→ Problem solved using the *MoveIt* implementation of the quaternion approach proposed by [13].

Hand-eye calibration results

Hand-eye calibration reprojection error

	<i>Nominal model</i>	<i>Calibrated model</i>
24 half-spheric poses $8 \times \frac{\pi}{3}, 8 \times \frac{\pi}{4}, 8 \times \frac{\pi}{6}$	2.0 mm - 0.0045 rad	1.9 mm - 0.0045 rad
48 half-spheric poses $16 \times \frac{\pi}{3}, 16 \times \frac{\pi}{4}, 16 \times \frac{\pi}{6}$	2.3 mm - 0.0055 rad	2.3 mm - 0.0056 rad
<i>Estimation "error"</i>	1.0 mm - 0.015 rad	1.2 mm - 0.013 rad

Results hard to compare...

- High sensitivity to **external parameters**:
- **Model and inverse kinematics** impact;
- **No ground truth data** about the hand-eye transformation.

Example of a robotized 3D scan

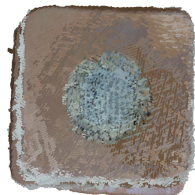


3D scan using an Intel Realsense D435 and an UR10e (speed $\times 3$)

First 3D scan results



ICP



RTABMAP (GraphSLAM)

First results obtained after the geometric characterization
10 point clouds, circular trajectory of latitude $\frac{\pi}{4}$ rad and radius 20 cm

Projected work and perspectives

- **Assess the actual impact of kinematic calibration on hand-eye calibration**
- **Define a reference and a metric to quantitatively evaluate the reconstruction quality**
 - ↪ Investigate reconstructions metrics depending on the nature of the generated data, and the relevant geometric objects [11][14].
- **Implement a more accurate and robust registration algorithm**
 - ↪ Use a more adequate sensor, such as the close-range *D405 Intel Realsense*.
 - ↪ Investigate mobile robotics and SLAM solutions;
- **Integrate real-time depth data to improve of the robot motion [15].**

Table of Contents

- 1 Introduction - Context and objectives
- 2 Robotic arm kinematic calibration - Accuracy improvement
- 3 Geometric characterization - 3D scan
- 4 Acoustic characterization - Acoustic field reconstruction
- 5 Conclusion & discussion

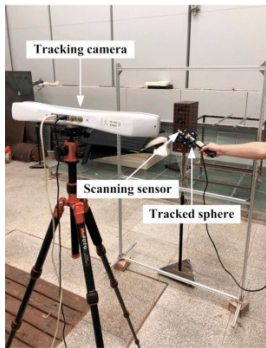
Acoustic characterization : context and motivation

→ **A shy use of robots in acoustics.**



Example of planar robotized acoustic measurements [16]

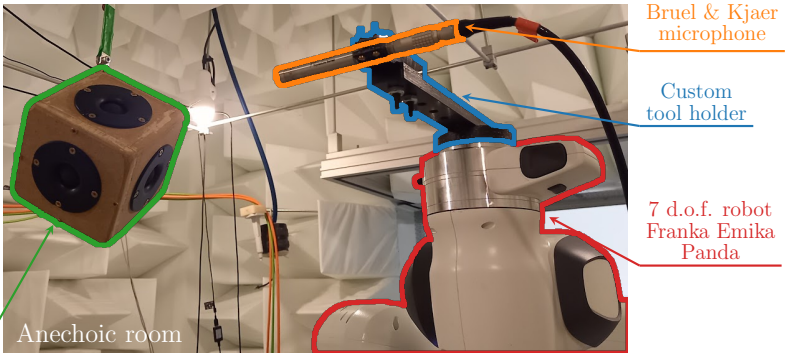
→ **An increasing need of high numbered 3D measurements.**



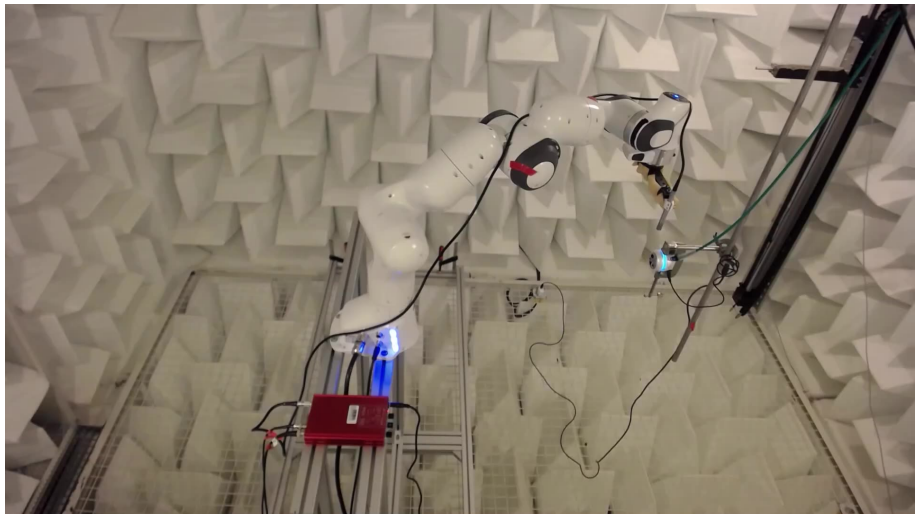
Example of 3D tracked acoustic measurements [2]

⇒ **Objective** : Reconstruct the acoustic field radiated by an unknown acoustic source.

Robotized acoustic measurements setup



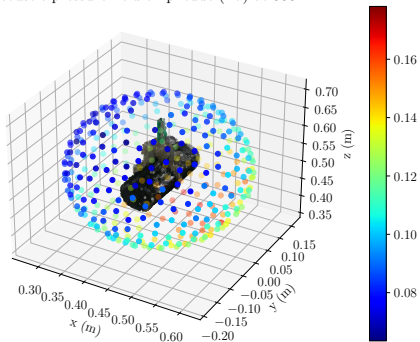
Example of robotized acoustic measurements



Acoustic directivity measurements using a Microflown PU probe and a Franka Panda in an Anechoïc chamber (speed $\times 2$)

First reconstruction results - Measurements

Acoustic pressure field amplitude (Pa) at 500 Hz



Acoustic pressure field phase (rad) at 500 Hz

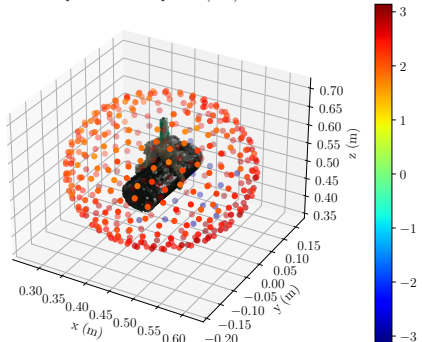


Figure 1: Sound pressure levels and phase measured at 500 Hz for each measured position

372 measurements, spherical mesh of radius 35 cm and resolution 5 cm

First reconstruction results - Boundary Elements Method

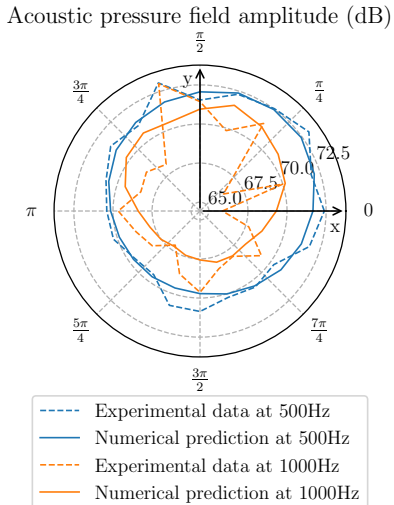


Figure 2: Predicted and measured sound pressure levels at 500 Hz and 1000 Hz
20 measurements, circular trajectory of latitude 0 rad and diameter 50 cm

First reconstruction results - Boundary Elements Method

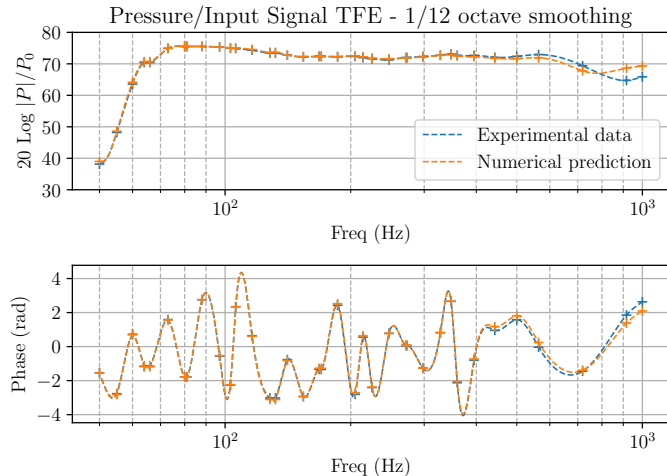


Figure 3: Predicted and measured data over the measurements frequential validity range
Measurement at a 0 rad longitude

Projected work and perspectives

- **Assess measurements and positioning uncertainties**
- **Reduce prediction errors at high frequencies**
 - ↪ Reduce the robot acoustic footprint using physical protections and smarter motion planning;
 - ↪ Perform close-range conformal measurements, and use high-order bended elements.
- **Investigate near-field acoustic holography opportunities**
 - ↪ Implement the dual near-field acoustic holography problem resolution;
 - ↪ Validate reconstructions using (robotized) displacement measurements !

Table of Contents

- 1 Introduction - Context and objectives
- 2 Robotic arm kinematic calibration - Accuracy improvement
- 3 Geometric characterization - 3D scan
- 4 Acoustic characterization - Acoustic field reconstruction
- 5 Conclusion & discussion

Thank you for your time and attention !

Caroline Pascal, Olivier Doaré, Alexandre Chapoutot, "A ROS-based kinematic calibration tool for serial robots", *IROS 2023 - IEEE/RSJ International Conference on Intelligent Robots and Systems*, Oct 2023, Detroit (MI), United States.



gitlab.ensta.fr/pascal.2020

References I

-  Pietro Li Volsi.
Aeroacoustic optimization of MAV rotors, 2023.
-  Zhong-Wei Luo, Daniel Fernandez Comesana, Chang-Jun Zheng, and Chuan-Xing Bi.
Near-field acoustic holography with three-dimensional scanning measurements.
Journal of Sound and Vibration, 2019.
-  Hanwen Bi, Fei Ma, Thushara D. Abhayapala, and Prasanga N. Samarasinghe.
Spherical array based drone noise measurements and modelling for drone noise reduction via propeller phase control.
In 2021 IEEE Workshop on Applications of Signal Processing to Audio and Acoustics (WASPAA), 2021.

References II

-  Caroline Pascal, Alexandre Chapoutot, and Olivier Doaré.
A ROS-based kinematic calibration tool for serial robots.
In *IEEE/RSJ International Conference on Intelligent Robots and Systems (IROS)*, 2023.
-  Yier Wu, Alexandr Klimchik, Stéphane Caro, Benoît Furet, and Anatol Pashkevich.
Geometric calibration of industrial robots using enhanced partial pose measurements and design of experiments.
Robotics and Computer-Integrated Manufacturing, 2015.
-  Hoai-Nhan Nguyen, Phu-Nguyen Le, and Hee-Jun Kang.
A performance comparison of the full pose- and partial pose-based robot calibration for various types of robot manipulators.
Advances in Mechanical Engineering, 2021.

References III



Anatol Pashkevich.

Computer-aided generation of complete irreducible models for robotic manipulators.

In *The 3rd Int. Conference of Modelling and Simulation*, 2001.



Luca Lattanzi, Cristina Cristalli, Daniele Massa, Sébastien Boria, Pierre Lépine, and Marcello Pellicciari.

Geometrical calibration of a 6-axis robotic arm for high accuracy manufacturing task.

The International Journal of Advanced Manufacturing Technology, 2020.



David Daney, Yves Papegay, and Blaise Madeline.

Choosing measurement poses for robot calibration with the local convergence method and tabu search.

The International Journal of Robotics Research, 2005.

References IV



Alexandr Klimchik, Yier Wu, Stéphane Caro, Benoît Furet, and Anatol Pashkevich.

Geometric and elastostatic calibration of robotic manipulator using partial pose measurements.

Advanced Robotics, 2014.



M. Callieri, A. Fasano, G. Impoco, P. Cignoni, R. Scopigno, G. Parrini, and G. Biagini.

RoboScan: an automatic system for accurate and unattended 3d scanning.

In *Proceedings of the 2nd International Symposium on 3D Data Processing, Visualization and Transmission*, 2004.

References V



Mathieu Labb  and Fran ois Michaud.

RTAB-map as an open-source lidar and visual simultaneous localization and mapping library for large-scale and long-term online operation.

Journal of Field Robotics, 2019.



Konstantinos Daniilidis.

Hand-Eye Calibration Using Dual Quaternions.

The International Journal of Robotics Research, 1999.



Petras Vestartas and Yves Weinand.

Laser scanning with industrial robot arm for raw-wood fabrication.

In *Proceedings of the 37th International Symposium on Automation and Robotics in Construction (ISARC)*, 2020.

References VI



Ji Seo, Inhwan Lee, and Byounghyun Yoo.

Effectiveness of rough initial scan for high-precision automatic 3d scanning.

Journal of Computational Design and Engineering, 2021.



Mélanie Nolan, Samuel Verburg, Jonas Brunskog, and Efren Fernandez-Grande.

Experimental characterization of the sound field in a reverberation room.

The Journal of the Acoustical Society of America, 2019.